ARTICLES

Search for charged Higgs boson decays of the top quark using hadronic τ decays

F. Abe,[14] H. Akimoto,[32] A. Akopian,[27] M. G. Albrow,[7] S. R. Amendolia,[23] D. Amidei,[17] J. Antos,[29] C. Anway-Wiese,[4] S. Aota,[32] G. Apollinari,[27] T. Asakawa,[32] W. Ashmanskas,[15] M. Atac,[7] P. Auchincloss,[26] F. Azfar,[22] P. Azzi-Bacchetta,[21] N. Bacchetta,[21] W. Badgett,[17] S. Bagdasarov,[27] M. W. Bailey,[19] J. Bao,[35] P. de Barbaro,[26] A. Barbaro-Galtieri,[15] V. E. Barnes,[25] B. A. Barnett,[13] G. Bauer,[16] T. Baumann,[9] F. Bedeschi,[23] S. Behrends,[3] S. Belforte,[23] G. Bellettini,[23] J. Bellinger,[34] D. Benjamin,[31] J. Benlloch,[16] J. Bensinger,[3] D. Benton,[22] A. Beretvas,[7] J. P. Berge,[7] J. Berryhill,[5] S. Bertolucci,[8] A. Bhatti,[27] K. Biery,[12] M. Binkley,[7] D. Bisello,[21] R. E. Blair,[1] C. Blocker,[3] A. Bodek,[26] W. Bokhari,[16] V. Bolognesi,[7] D. Bortoletto,[25] J. Boudreau,[24] L. Breccia,[2] C. Bromberg,[18] N. Bruner,[19] E. Buckley-Geer,[7] H. S. Budd,[26] K. Burkett,[17] G. Busetto,[21] A. Byon-Wagner,[7] K. L. Byrum,[1] J. Cammerata,[13] C. Campagnari,[7] M. Campbell,[17] A. Caner,[7] W. Carithers,[15] D. Carlsmith,[34] A. Castro,[21] D. Cauz,[23] Y. Cen,[26] F. Cervelli,[23] H. Y. Chao,[29] J. Chapman,[17] M.-T. Cheng,[29] G. Chiarelli,[23] T. Chikamatsu,[32] C. N. Chiou,[29] L. Christofek,[11] S. Cihangir,[7] A. G. Clark,[23] M. Cobal,[23] M. Contreras,[5] J. Conway,[28] J. Cooper,[7] M. Cordelli,[8] C. Couyumtzelis,[23] D. Crane,[1] D. Cronin-Hennessy,[6] R. Culbertson,[5] J. D. Cunningham,[3] T. Daniels,[16] F. DeJongh,[7] S. Delchamps,[7] S. Dell'Agnello,[23] M. Dell'Orso,[23] L. Demortier,[27] B. Denby,[23] M. Deninno,[2] P. F. Derwent,[17] T. Devlin,[28] M. Dickson,[26] J. R. Dittmann,[6] S. Donati,[23] J. Done,[30] T. Dorigo,[21] A. Dunn,[17] N. Eddy,[17] K. Einsweiler,[15] J. E. Elias,[7] R. Ely,[15] E. Engels, Jr.,[24] D. Errede,[11] S. Errede,[11] Q. Fan,[26] I. Fiori,[2] B. Flaugher,[7] G. W. Foster,[7] M. Franklin,[9] M. Frautschi,[31] J. Freeman,[7] J. Friedman,[16] H. Frisch,[5] T. A. Fuess,[1] Y. Fukui,[14] S. Funaki,[32] G. Gagliardi,[23] S. Galeotti,[23] M. Gallinaro,[21] M. Garcia-Sciveres,[15] A. F. Garfinkel,[25] C. Gay,[9] S. Geer,[7] D. W. Gerdes,[17] P. Giannetti,[23] N. Giokaris,[27] P. Giromini,[8] L. Gladney,[22] D. Glenzinskí,[13] M. Gold,[19] J. Gonzalez,[22] A. Gordon,[9] A. T. Goshaw,[6] K. Goulianos,[27] H. Grassmann,[23] L. Groer,[28] C. Grosso-Pilcher,[5] G. Guillian,[17] R. S. Guo,[29] C. Haber,[15] E. Hafen,[16] S. R. Hahn,[7] R. Hamilton,[9] R. Handler,[34] R. M. Hans,[35] K. Hara,[32] A. D. Hardman,[25] B. Harral,[22] R. M. Harris,[7] S. A. Hauger,[6] J. Hauser,[4] C. Hawk,[28] E. Hayashi,[32] J. Heinrich,[22] K. D. Hoffman,[25] M. Hohlmaan,[1,5] C. Holck,[22] R. Hollebeek,[22] L. Holloway,[11] A. Hölscher,[12] S. Hong,[17] G. Houk,[22] P. Hu,[24] B. T. Huffman,[24] R. Hughes,[26] J. Huston,[18] J. Huth,[9] J. Hylen,[7] H. Ikeda,[32] M. Incagli,[23] J. Incandela,[7] G. Introzzi,[23] J. Iwai,[32] Y. Iwata,[10] H. Jensen,[7] U. Joshi,[7] R. W. Kadel,[15] E. Kajfasz,[7] T. Kamon,[30] T. Kaneko,[32] K. Karr,[33] H. Kasha,[35] Y. Kato,[20] L. Keeble,[8] K. Kelley,[16] R. D. Kennedy,[28] R. Kephart,[7] P. Kesten,[15] D. Kestenbaum,[9] R. M. Keup,[11] H. Keutelian,[7] F. Keyvan,[4] B. Kharadia,[11] B. J. Kim,[26] D. H. Kim,[7,*] H. S. Kim,[12] S. B. Kim,[17] S. H. Kim,[32] Y. K. Kim,[15] L. Kirsch,[3] P. Koehn,[26] K. Kondo,[32] J. Konigsberg,[9] S. Kopp,[5] K. Kordas,[12] W. Koska,[7] E. Kovacs,[7,*] W. Kowald,[6] M. Krasberg,[17] J. Kroll,[7] M. Kruse,[25] T. Kuwabara,[32] S. E. Kuhlmann,[1] E. Kuns,[28] A. T. Laasanen,[25] N. Labanca,[23] S. Lammel,[7] J. I. Lamoureux,[3] T. LeCompte,[11] S. Leone,[23] J. D. Lewis,[7] P. Limon,[7] M. Lindgren,[4] T. M. Liss,[11] N. Lockyer,[22] O. Long,[22] C. Loomis,[28] M. Loreti,[21] J. Lu,[30] D. Lucchesi,[23] P. Lukens,[7] S. Lusin,[34] J. Lys,[15] K. Maeshima,[7] A. Maghakian,[27] P. Maksimovic,[16] M. Mangano,[23] J. Mansour,[18] M. Mariotti,[21] J. P. Marriner,[7] A. Martin,[11] J. A. J. Matthews,[19] R. Mattingly,[16] P. McIntyre,[30] P. Melese,[27] A. Menzione,[23] E. Meschi,[23] S. Metzler,[22] C. Miao,[17] G. Michail,[9] R. Miller,[18] H. Minato,[32] S. Miscetti,[8] M. Mishina,[14] H. Mitsushio,[32] T. Miyamoto,[32] S. Miyashita,[32] Y. Morita,[14] J. Mueller,[24] A. Mukherjee,[7] T. Muller,[4] P. Murat,[23] H. Nakada,[32] I. Nakano,[32] C. Nelson,[7] D. Neuberger,[4] C. Newman-Holmes,[7] M. Ninomiya,[32] L. Nodulman,[1] S. H. Oh,[6] K. E. Ohl,[35] T. Ohmoto,[10] T. Ohsugi,[10] R. Oishi,[32] M. Okabe,[32] T. Okusawa,[20] R. Oliver,[22] J. Olsen,[34] C. Pagliarone,[2] R. Paoletti,[23] V. Papadimitriou,[31] S. P. Pappas,[35] S. Park,[7] A. Parri,[8] J. Patrick,[7] G. Pauletta,[23] M. Paulini,[15] A. Perazzo,[23] L. Pescara,[21] M. D. Peters,[15] T. J. Phillips,[6] G. Piacentino,[2] M. Pillai,[26] K. T. Pitts,[7] R. Plunkett,[7] L. Pondrom,[34] J. Proudfoot,[1] F. Ptohos,[9] G. Punzi,[23] K. Ragan,[12] A. Ribon,[21] F. Rimondi,[2] L. Ristori,[23] W. J. Robertson,[6] T. Rodrigo,[7,*] S. Rolli,[23] J. Romano,[5] L. Rosenson,[16] R. Roser,[11] W. K. Sakumoto,[26] D. Saltzberg,[5] A. Sansoni,[8] L. Santi,[23] H. Sato,[32] V. Scarpine,[30] P. Schlabach,[9] E. E. Schmidt,[7] M. P. Schmidt,[35] A. Scribano,[23] S. Segler,[7] S. Seidel,[19] Y. Seiya,[32] G. Sganos,[12] A. Sgolacchia,[2] M. D. Shapiro,[15] N. M. Shaw,[25] Q. Shen,[25] P. F. Shepard,[24] M. Shimojima,[32] M. Shochet,[5] J. Siegrist,[15] A. Sill,[31] P. Sinervo,[12] P. Singh,[24] J. Skarha,[13] K. Sliwa,[33] F. D. Snider,[13] T. Song,[17] J. Spalding,[7] P. Sphicas,[16] F. Spinella,[23] M. Spiropulu,[9] L. Spiegel,[7] L. Stanco,[21] J. Steele,[34] A. Stefanini,[23] K. Strahl,[12] J. Strait,[7] R. Ströhmer,[9] D. Stuart,[7] G. Sullivan,[5] A. Soumarokov,[29] K. Sumorok,[16] J. Suzuki,[32] T. Takada,[32] T. Takahashi,[20] T. Takano,[32] K. Takikawa,[32] N. Tamura,[10] F. Tartarelli,[23] W. Taylor,[12] P. K. Teng,[29] Y. Teramoto,[20] S. Tether,[16] D. Theriot,[7] T. L. Thomas,[19] R. Thun,[17] M. Timko,[33] P. Tipton,[26] A. Titov,[27] S. Tkaczyk,[7] D. Toback,[5] K. Tollefson,[26] A. Tollestrup,[7] J. Tonnison,[25] J. F. de Troconiz,[9] S. Truitt,[17] J. Tseng,[13] N. Turini,[23] T. Uchida,[32] N. Uemura,[32] F. Ukegawa,[22] G. Unal,[22] S. C. van den Brink,[24] S. Vejcik, III,[17] G. Velev,[23] R. Vidal,[7] M. Vondracek,[11] D. Vucinic,[16] R. G. Wagner,[1] R. L. Wagner,[7] J. Wahl,[5] C. Wang,[6] C. H. Wang,[29] G. Wang,[23] J. Wang,[5] M. J. Wang,[29] Q. F. Wang,[27] A. Warburton,[12] G. Watts,[26] T. Watts,[28] R. Webb,[30] C. Wei,[6] C. Wendt,[34] H. Wenzel,[15] W. C. Wester, III,[7] A. B. Wicklund,[1] E. Wicklund,[7] R. Wilkinson,[22] H. H. Williams,[22] P. Wilson,[5] B. L. Winer,[26] D. Wolinski,[17] J. Wolinski,[30] X. Wu,[23] J. Wyss,[21] A. Yagil,[7] W. Yao,[15] K. Yasuoka,[32] Y. Ye,[12] G. P. Yeh,[7] P. Yeh,[29] M. Yin,[6] J. Yoh,[7] C. Yosef,[18] T. Yoshida,[20] D. Yovanovitch,[7] I. Yu,[35] L. Yu,[19] J. C. Yun,[7] A. Zanetti,[23] F. Zetti,[23] L. Zhang,[34] W. Zhang,[22] and S. Zucchelli[2]

(CDF Collaboration)

0556-2821/96/54(1)/735(8)/$10.00

[1]*Argonne National Laboratory, Argonne, Illinois 60439*
[2]*Istituto Nacionale de Fisica Nucleare, University of Bologna, I-40126 Bologna, Italy*
[3]*Brandeis University, Waltham, Massachusetts 02254*
[4]*University of California at Los Angeles, Los Angeles, California 90024*
[5]*University of Chicago, Chicago, Illinois 60637*
[6]*Duke University, Durham, North Carolina 27708*
[7]*Fermi National Accelerator Laboratory, Batavia, Illinois 60510*
[8]*Laboratori Nacionali di Frascati, Istituto Nazionale di Fisica Nucleare, I-00044 Frascati, Italy*
[9]*Harvard University, Cambridge, Massachusetts 02138*
[10]*Hirashima University, Higashi-Hiroshima 724, Japan*
[11]*University of Illinois, Urbana, Illinois 61801*
[12]*Institute of Particle Physics, McGill University, Montreal H3A 2TS, and University of Toronto, Toronto M5S 1A7, Canada*
[13]*The Johns Hopkins University, Baltimore, Maryland 21218*
[14]*National Laboratory for High Energy Physics (KEK), Tsukuba, Ibaraki 305, Japan*
[15]*Lawrence Berkeley Laboratory, Berkeley, California 94720*
[16]*Massachusetts Institute of Technology, Cambridge, Massachusetts 02139*
[17]*University of Michigan, Ann Arbor, Michigan 48109*
[18]*Michigan State University, East Lansing, Michigan 48824*
[19]*University of New Mexico, Albuquergue, New Mexico 87131*
[20]*Osaka City University, Osaka 588, Japan*
[21]*Universita di Padova, Istituto Nazionale di Fisica Nucleare, Sezione di Padova, I-35131 Padova, Italy*
[22]*University of Pennsylvania, Philadelphia, Pennsylvania 19104*
[23]*Istituto Nazionale di Fisica Nucleare, University and Scuola Normale Superiore of Pisa. I-56100 Pisa, Italy*
[24]*University of Pittsburgh, Pittsburgh, Pennsylvania 15260*
[25]*Purdue University, West Lafayette, Indiana 47907*
[26]*University of Rochester, Rochester, New York 14627*
[27]*Rockefeller University, New York, New York 10021*
[28]*Rutgers University, Piscataway, New Jersey 08454*
[29]*Academia Sinira, Taipei, Taiwan 11529, Republic of China*
[30]*Texas A&M University, College Station, Texas 27843*
[31]*Texas Tech University, Lubbock, Texas 79409*
[32]*University of Tsukuba, Tsukuba, Ibaraki 305, Japan*
[33]*Tufts University, Medford, Massachusetts 02155*
[34]*University of Wisconsin, Madison, Wisconsin 53706*
[35]*Yale University, New Haven, Connecticut 06511*

(Received 10 January 1996)

We present the result of a search for charged Higgs boson decays of the top quark, produced in $p\bar{p}$ collisions at $\sqrt{s}=1.8$ TeV. When the charged Higgs boson is heavy and decays to a τ lepton, which subsequently decays hadronically, the resulting events have a unique signature: large missing transverse energy and the low-charged-multiplicity τ. Data collected in 1992 and 1993 at the Collider Detector at Fermilab, corresponding to 18.7 ± 0.7 pb^{-1}, exclude new regions of combined top quark and charged Higgs boson mass, in extensions to the standard model with two Higgs doublets.

PACS number(s): 14.65.Ha, 13.85.Rm

I. INTRODUCTION

We have conducted a search for decays of the top quark to a charged Higgs boson, using the Higgs boson decays to hadronically decaying τ leptons. The results presented here come from data collected during the years 1992 and 1993 at the Collider Detector at Fermilab corresponding to an integrated luminosity of 18.7 ± 0.7 pb^{-1}. A charged Higgs boson arises in extensions to the Standard Model with two Higgs doublets [1]. If the charged Higgs boson exists in such a model and is lighter than the top quark, then two competing channels are possible: $t\to H^+b$ and $t\to W^+b$. The charged Higgs boson can decay either to $\tau\bar{\nu}$ or to $c\bar{s}$. The branching ratios of these processes depend on the top quark and charged Higgs masses, and on $\tan\beta$, the ratio of the vacuum expectation values of the two Higgs doublets in the model.[1] We consider here only the kinematically allowed cases where $m_{\rm top}>m_H+m_b$ and $m_{\rm top}>m_W+m_b$. In these cases three decay modes of the quark pairs are possible: $t\bar{t}\to H^+H^-b\bar{b}$, $t\bar{t}\to H^\pm W^\mp b\bar{b}$, and $t\bar{t}\to W^+W^-b\bar{b}$.

This analysis of hadronic decays of the τ lepton uses a method similar to that used previously [2] but with four

*Visitor.

[1]We consider here only models in which one Higgs doublet couples to the up-type quarks, and the other doublet couples to the down-type quarks and the leptons.

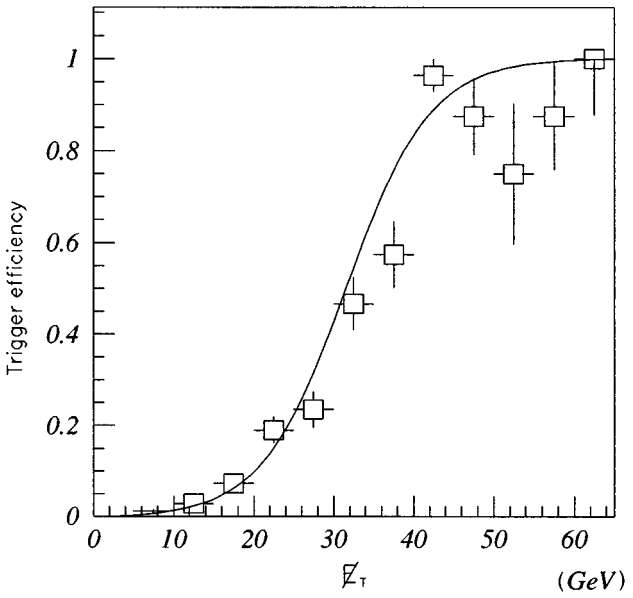

FIG. 1. Distribution of measured trigger efficiency as a function of reconstructed $\not\!\!E_T$ in jet trigger events.

times more integrated luminosity and an event selection designed for larger top and charged Higgs boson masses. Our most recent limit [3] uses the leptonic decays of the τ using the data set collected in the same period as in this paper, i.e., 1992-1993. Charged Higgs boson masses from 45 GeV/c^2 to 110 GeV/c^2 and top quark masses from 90 GeV/c^2 to 110 GeV/c^2 were excluded at a 95% C.L., as shown in the lower hatched part of the plot in Fig. 7. Experiments at the CERN e^+e^- collider LEP exclude a charged Higgs boson with a mass less than 45 GeV/c^2 [4].

In the present analysis a more stringent limit results from the 64% hadronic branching ratio of the τ, compared with the 36% leptonic branching ratio. However, the larger expected background, mainly hadronic processes, must be well modeled. The analysis presented here addresses top masses in the range extending from the limits of previous searches [2,3], about 100 GeV/c^2, up to the mass range which has been measured, 176 ± 8(stat)±10(syst) GeV/c^2 [5]. The analysis excludes by direct search a top or top-like object decaying via a charged Higgs boson in this region.

Top quark pair events with one or two charged Higgs boson decays should contain energetic jets which come from b quarks and the decays of the τ's. Each top quark leads to the production of two energetic neutrinos, leading in turn to a large missing transverse energy, denoted $\not\!\!E_T$.[2] The first neutrino is emitted in the charged Higgs or W boson decay, and the second results from the τ decay. The signature of an hadronically decaying τ is a narrow jet with either one or three associated charged particles. Thus, top quark pair events with charged Higgs decays to τ leptons can be found by looking for an excess of events with narrow energetic jets with one or three charged particles coming from the τ, along with the presence of other energetic hadronic jets and neutrinos. This signature differs from that of standard model top events due to the higher probability of decays to τ leptons, and larger missing E_T.

[2]For a calorimeter energy deposit, assuming the particles came from some point along the beam axis, a direction in space is defined. The transverse energy E_T is the component of the energy vector in the plane perpendicular to the beam axis. The $\not\!\!E_T$ is defined as the magnitude of the vector sum of the transverse energy E_T of each calorimeter energy deposit.

TABLE I. Number of events selected and signal efficiency for each selection criterion. The efficiencies represent the successive effect of each criterion, for events in a Monte Carlo simulation with $m_{\rm top}=120$ GeV/c^2 and $m_{\rm Higgs}=100$ GeV/c^2.

Cuts	Remaining Events	Relative Efficiency
Initial selection	7109	$(22.2\pm0.4))$%
$E_T>40$ GeV	4766	(85.8 ± 0.8)%
Jet 1 $E_T>30$ GeV	2579	(83.5 ± 0.8)%
Jet 2 $E_T>20$ GeV	1601	(81.6 ± 1.0)%
Azimuthal angle between jets	1579	$100.0^{+0.0}_{-0.1}$%
$S(E_T)>4$ GeV$^{1/2}$	659	(79.7 ± 1.1)%
Isolation	193	(48.9 ± 1.6)%
Electron/jet rejection	104	(93.4 ± 1.1)%
Δz vertex	81	$100.0^{+0.0}_{-0.2}$%
$\Sigma\lvert E_T\rvert>100$ GeV	74	(93.3 ± 1.2)%
Charged multiplicity	19	(88.6 ± 1.5)%
Total efficiency		(3.9 ± 0.2)%

II. CDF DETECTOR AND TRIGGER

The CDF detector is described in detail elsewhere [6]. The most important components of the CDF detector for this analysis are the tracking chambers and calorimeters. The relevant tracking chambers are the vertex time projection chamber (VTX) and the central tracking chamber (CTC), which is a large cylindrical drift chamber surrounding the VTX. Both are located inside a superconducting solenoid magnet generating a 1.4 T field. The VTX provides z vertex reconstruction and $r-z$ tracking over the pseudorapidity range $\lvert\eta\rvert<3.25$ [7], where the z axis is the proton direction along the beamline and r refers to the radial coordinate transverse to the beam line. The momenta of charged particles are measured in the CTC. The solenoid and the tracking volume of the CDF lie inside electromagnetic and hadronic calorimeters which cover 2π in azimuth and up to $\lvert\eta\rvert=4.2$. The calorimeters are segmented in azimuth and pseudorapidity to form a tower geometry which points back to the nominal interaction point $z=0$.

The ''trigger'' decision as to whether or not the data from a particular interaction should be recorded depends on the particular pattern of energy deposited in the calorimeters, the presence of charged tracks in the CTC, and the presence of penetrating charged particles in the muon chambers which surround the calorimeter. This analysis relies in particular on a trigger which uses analog sums of the calorimeter energy deposits to determine the missing transverse energy. Since the charged Higgs boson events sought in this analysis generally have large missing transverse energy, this analysis uses only those events which satisfy a trigger requirement of

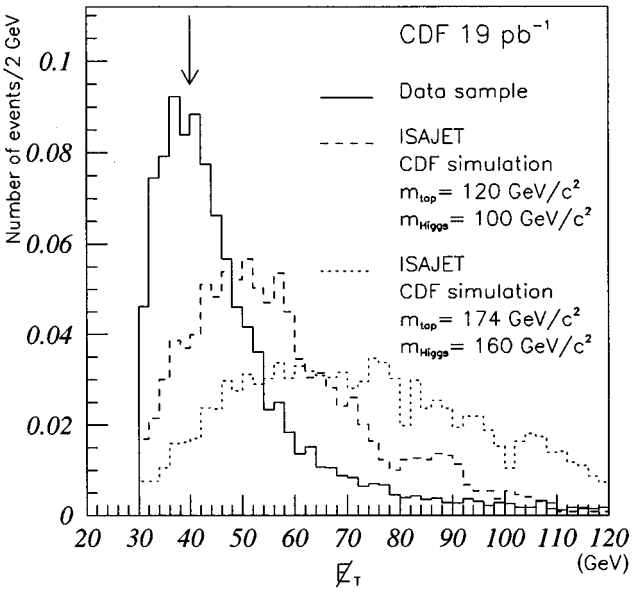

FIG. 2. Distribution of $\not\!\!E_T$ for the data sample (solid line) and for the Monte Carlo simulation (dashed and dotted lines). Events to the left of the arrow are removed by the cuts on the data sample.

at least 35 GeV of missing transverse energy.

Figure 1 shows the trigger efficiency measured from the data as a function of the reconstructed missing energy. The imperfect missing energy resolution in the trigger electronics leads to the measured shape of the ''turn-on'' at 35 GeV. The trigger attains full efficiency at about $\not\!\!E_T$=60 GeV.

III. EVENT SELECTION

The criteria to reject background and to select the charged Higgs boson signal were determined using a Monte Carlo

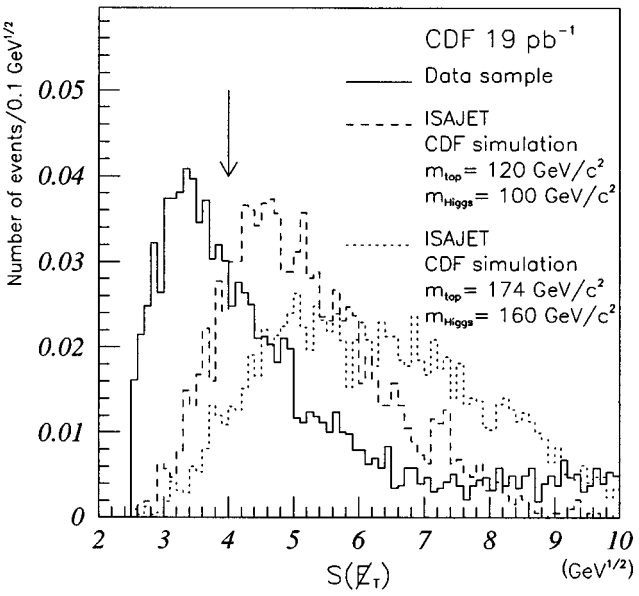

FIG. 3. Distribution of $S(\not\!\!E_T)$ for the data sample (solid line) and for the Monte Carlo simulations (dashed and dotted line). Events to the left of the arrow are removed by the cut.

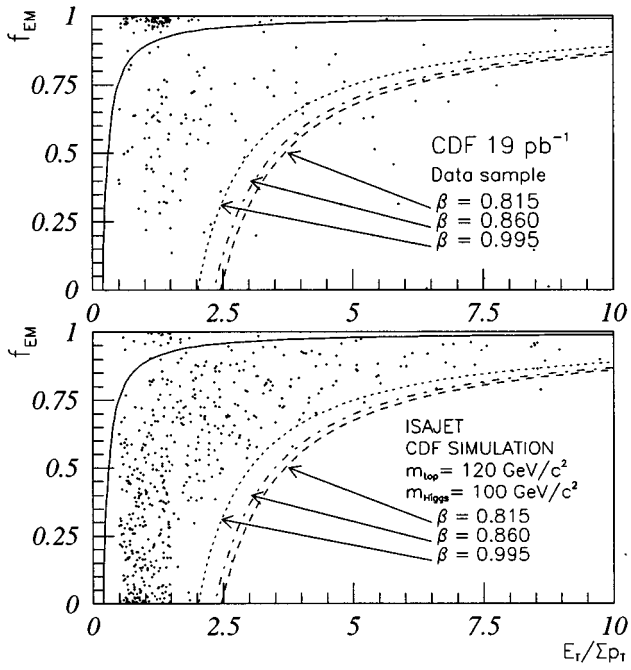

FIG. 4. Distibution of electromagnatic energy fraction versus $E_T/\Sigma p_T$, showing electron and hadronic jet rejection limits.

simulation based on top quark and charged Higgs boson masses just beyond those excluded in previous analyses, namely, $m_{\rm top}$=120 GeV/c^2 and $m_{\rm Higgs}$=100 GeV/c^2. A version of the Monte Carlo program ISAJET [8], modified to correctly model the polarization of the τ's, generated events which were then passed through the CDF detector simulation.

The selection criteria aim to select events with large missing transverse energy due to the neutrinos the presence of a hadronically decaying τ lepton, and at least one other jet due either to another τ or to one of the jets from the top quark. Each event must have $\not\!\!E_T$>40 GeV, $S(\not\!\!E_T)$>4 GeV$^{1/2}$, a τ lepton identified as discussed below, with E_T>30 GeV and $|\eta|$<1, a jet as defined below, with E_T>20 GeV, $|\eta|$<2, $\Delta\phi_{\tau\text{-jet}}$<140°, and scalar $\Sigma|E_T|$>100 GeV, where we use the definition $S(\not\!\!E_T)\equiv\not\!\!E_t/\sqrt{\Sigma|E_T|}$ for the ''significance'' of the missing E_T.

The number of events which satisfy each criterion are listed in Table I. The relative efficiencies between consecutive cuts for the ISAJET Monte Carlo simulation with $m_{\rm top}$=120 GeV/c^2 and $m_{\rm Higgs}$=100 GeV/c^2 are also shown in Table I.

The scalar nature of the charged Higgs boson implies that the two neutrinos produced in the decay chain tend to travel in the same direction, resulting in a large $\not\!\!E_T$. Furthermore, the charged Higgs boson decays mainly to a τ for large values of the parameter tan β. For smaller tan β values, the probability for the top quark to decay to a W boson increases, and the charged Higgs boson decays more often to a quark-antiquark pair. In this case the average $\not\!\!E_T$ consequently becomes smaller. Thus the trigger and selection requirements on $\not\!\!E_T$ enhance the acceptance in the case of large values of tan β.

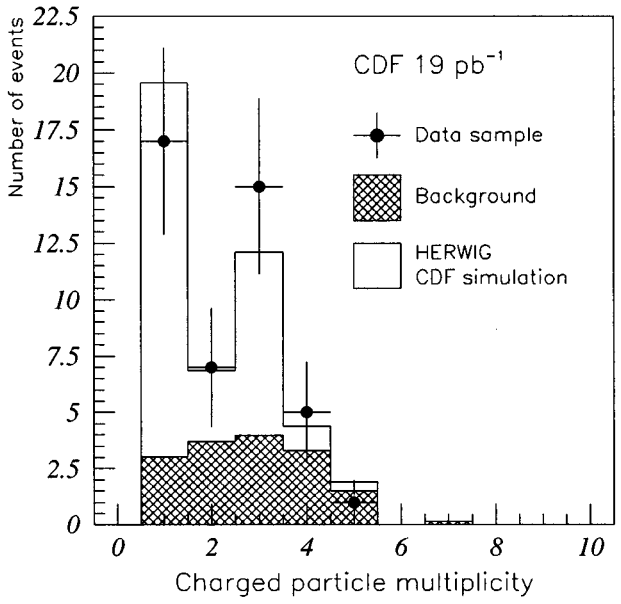

FIG. 5. The τ signal found in the data sample using a similar algorithm with less stringent cuts. The data (points) are compared with an estimate of jet background (crosshatched), and with a Monte Carlo simulation of W+jets events, with $W\rightarrow\tau\nu$ (open histogram).

The criteria on the missing transverse energy and significance reinforce the trigger requirements and select events with energetic neutrinos. The distributions of $\not\!\!E_T$ and $S(\not\!\!E_T)$ are shown in Figs. 2 and 3, for the data sample and for the Monte Carlo simulation of the signal.

When a top quark decays to a charged Higgs boson, a large fraction of its energy goes into creation of the charged Higgs boson. The smaller remaining energy for the b quark produces jets of lower E_T. Since the charged Higgs boson carries a large energy, its decay products receive a strong boost. In particular, the τ's which come from the charged Higgs boson have very large E_T, resulting in a large-transverse-momentum (p_T) associated charged particle near the jet axis. The average p_T increases with increasing charged Higgs mass. A charged particle is associated with a jet if its initial direction points within a cone of radius $\Delta R=\sqrt{\Delta\eta^2+\Delta\phi^2}=0.4$ of the jet direction, where ϕ is the azimuthal angle in the plane perpendicular to the beam axis.

The event selection requires the presence of at least two jets, formed from calorimeter energy deposits in a cone of radius $\Delta R=0.4$. The first jet must have $E_T>30$ GeV, lie in the region $|\eta|<1$, and have an associated charged particle with $p_T>4$ GeV/c. If more than one jet satisfies these criteria, the jet with the largest E_T is chosen.

The requirements on the second jet are less stringent. The Monte Carlo simulation shows that the second jet has a smaller E_T, and is less often in the central region of the detector, $|\eta|<1$. The second jet must have $E_T>20$ GeV, $|\eta|<2$, and an associated charged particle.

Requiring that the z intercept of the largest-p_T charged particle associated with each jet be within 5 cm of the primary z vertex of the event rejects jets from additional interactions in the event.

Subsequent criteria to identify hadronically decaying τ's assign one of the two jets as the ''τ.'' Since the charged particles in hadronically decaying energetic τ's must lie in a narrow cone around the calorimeter energy deposit, the τ must satisfy an isolation criterion in which there must be no associated charged particle with $p_T>1$ GeV/c found between cones of 10° and 30° defined around the direction of the associated track with the largest p_T. If the first jet fails the cut, the algorithm applies the cut to the second jet, which in addition must then pass the stricter jet E_T, associated charged particle p_T, and η cuts of the first jet. The jet which passes the isolation cut is called the τ candidate. Applying this requirement after all the other requirements rejects 78% of the events in the data sample, while retaining 60% of the events in the Monte Carlo simulation with $m_{\rm top}=120$ GeV/c^2 and $m_{\rm Higgs}=100$ GeV/c^2.

A small fraction of electrons and single hadrons or low-multiplicity hadronic jets also satisfy the τ selection criteria. To reject electrons, the τ candidate must satisfy $1-(10E_T/\Sigma|p_T|-1)^{-1}>f_{\rm EM}$, where $f_{\rm EM}$ is the fraction of the total energy deposited in the electromagnetic calorimeter and $\Sigma|p_T|$ is the sum of the magnitudes of the transverse momenta of charged particles in the 10° cone around the jet axis. A fraction of the hadronic background is rejected by a similar cut: $1-(bE_T/\Sigma p_T-1)^{-1}<f_{\rm EM}$, where the factor b has been optimized as a function of the E_T of the τ candidate: $b=0.815$ for 30 GeV$\leqslant E_T<45$ GeV, $b=0.995$ for 45 GeV$\leqslant E_T<69$ GeV, and $b=0.860$ for $E_T\geqslant 69$ GeV.

Figure 4 shows the distribution of $f_{\rm EM}$ versus $E_T/\Sigma p_T$; the selection criteria appear as the curves drawn on the plot.

Lastly, the requirement that the scalar sum of transverse energy exceeds 100 GeV removes background from W+jets events in which the W decays leptonically.

IV. τ SIGNAL IN HADRONIC EVENTS

In order to demonstrate that the criteria select hadronic τ decays in a process known to contain τ leptons, one can extract the τ signal from the process $p\bar{p}\rightarrow W$+jets. $W\rightarrow\tau\nu$ by selecting a sample of events with a τ, a jet, and missing transverse energy. Employing less stringent cuts on the $\not\!\!E_T$, $S(\not\!\!E_T)$, E_T, and p_T of the charged particles associated with the jets, and then requiring $\Sigma|E_T|<85$ GeV and a tight cut on the width of the energy deposit in the jets, results in the multiplicity distribution shown in Fig. 5. The plot shows a clear excess of one and three charged particles in the distribution of the associated charged particle multiplicity distribution in the 10° cone, attributed to W plus jets events. The data (points) are compared to a background estimate (crosshatched histogram), and a HERWIG Monte Carlo simulation [9] of $W\rightarrow\tau\nu$ (open histogram), normalized according to the HERWIG predicted cross section.

V. MONTE CARLO SIMULATION AND TRIGGER EFFICIENCY

The simulation of charged Higgs boson events uses the physics generator ISAJET and the CDF detector simulation. In order to compute the acceptance at any point in the top quark versus charged Higgs boson mass plane, it is necessary to make a mixture of events from the simulation of $t\bar{t}\rightarrow H^+H^-bb$, $t\bar{t}\rightarrow H^\pm W^\mp bb$, and $t\bar{t}-W^+W^-bb$ processes

TABLE II. Sources and magnitudes of the systematic uncertainties in the analysis. The values are the relative uncertainties in the number of expected events, and represent the extremes for the top mass range 100–174 GeV/c^2.

Uncertainty	Value
Top quark cross section	(30–10)%
ISAJET gluon radiation	(16–1.3)%
Integrated luminosity	3.7%
Trigger efficiency	5.5%
MC statistics	(10–4)%
Energy scale effect	(32–7.5)%
Background estimation	14%

for charged Higgs boson masses in the range of 50 GeV/c^2–160 GeV/c^2 and for top quark masses in the range of 100 GeV/c^2–174 GeV/c^2. The $t\bar{t}$ production cross section is taken from a next-to-leading order theoretical calculation [10]. The simulation of the effect of the $\not\!\!E_T$ trigger efficiency comes from a measurement of the efficiency as a function of the $\not\!\!E_T$ in events which triggered on the presence of jets.

In the Monte Carlo simulation, more than 95% of τ candidates found by the algorithm correspond in spatial direction to the actual τ's generated in the event.

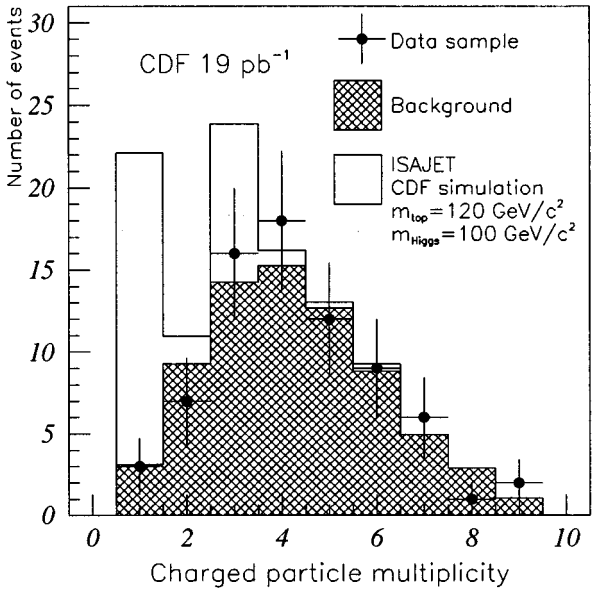

FIG. 6. Charged particle multiplicity distribution in the 10° cone after all the cuts, for the data sample (points), for the background normalized to the data (crosshatched histogram), and for the expected signal from the normalized Monte Carlo simulations (open histogram), added to the background.

VI. BACKGROUNDS

The dominant backgrounds to charged Higgs boson events in the selected event sample are hadronic processes, and processes in which a Z or W is produced, possibly accompanied by jets. In almost all of the background, a hadronic jet fluctuates to have low charged particle multiplicity and satisfies the τ criteria. A small additional contribution to the background comes from W and Z events where the τ jet comes from a τ or mismeasured electron from the boson decay. In this case the τ jet typically has one or three associated charged tracks.

A combination of events satisfying the various jet energy triggers in the experiment models the hadronic background well. The background normalization is computed as a function of the E_T and charged multiplicity of the τ. The normalization equalizes the number of events of any charged multiplicity except 1 or 3, in three ranges of E_T. The Monte Carlo simulation shows that real τ's contribute less than a few percent to these bins in multiplicity. An estimated total of 17.4 ± 2.5 events come from processes where the τ jet came from a hadronic jet; the error is statistical only.

The estimate of the non-hadronic-jet contribution to the background comes from Monte Carlo simulation of the various processes. Of these, only the contribution from $Z \rightarrow \tau^+\tau^-$ remains non-negligible after all cuts. Using a total of 30 000 events generated with the ISAJET program and then passed through the CDF detector simulation and analysis, we expect 1.1 ± 0.4(stat) events with 1 or 3 associated charged particles. The production cross section comes from the measured Z cross section, assuming lepton universality: $\sigma(p\bar{p} \rightarrow ZX : Z \rightarrow e^+e^-X) = 0.209 \pm 0.013\,(\text{stat}) \pm 0.017\,(\text{syst})$ nb [11]. This background is small for several reasons: the process has a small cross section, the two outgoing τ's are azimuthally back to back, and the $\not\!\!E_T$ is typically not large since the τ decay neutrinos are back to back.

The predicted background from W+jets events, with $W \rightarrow \tau\nu$, comes from 40 000 HERWIG events which were passed through the CDF detector simulation, including the relevant trigger efficiencies. Again assuming lepton universality the production cross section $\sigma(p\bar{p} \rightarrow WX : W \rightarrow e\nu) = 2.19 \pm 0.04(\text{stat}) \pm 0.21(\text{syst})$ nb [11] is used for normalization. Most of these events are rejected by the cuts on $\not\!\!E_T$, $S(\not\!\!E_T)$, and $\Sigma|e_T|$. No event passed the selection criteria.

The other processes involving W and Z bosons result in background taken into account by the hadronic jet sample, and contribute negligibly to the non-hadronic-jet component.

There is a small acceptance for events from standard model top quark pair production: for a top quark with mass of 176 GeV/c^2 one expects 0.2 ± 0.1(stat) events. This acceptance affects the number of expected events in the signal, and does not enter the background estimate.

VII. SYSTEMATIC UNCERTAINTIES

Systematic effects which can lead to uncertainty in the final result can be classified into those which affect the background estimate and those which affect the number of expected events. Many of the systematic uncertainties affecting the number of expected events depend on the top quark mass. Table II lists the different estimated systematic uncertainties. For the cases where there exists a top quark mass dependence, the extreme values appear in the table.

Various effects can bias the background estimation, such as the binning of the E_T distribution and the normalization method. Dividing the E_T distribution into smaller bins and following the same normalization method leads to a negligibly small difference in the expected number of hadronic

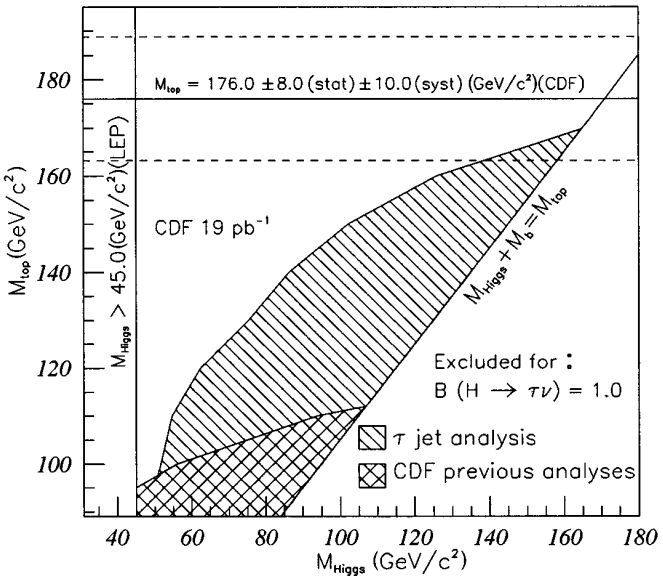

FIG. 7. Regions of the $(m_{\text{top}}, m_{\text{Higgs}})$ plane excluded at 95% C.L. for a 100% branching ratio of $H^{\pm} \rightarrow \tau\nu$. The plot also shows the limit from the previous analyses [2,3].

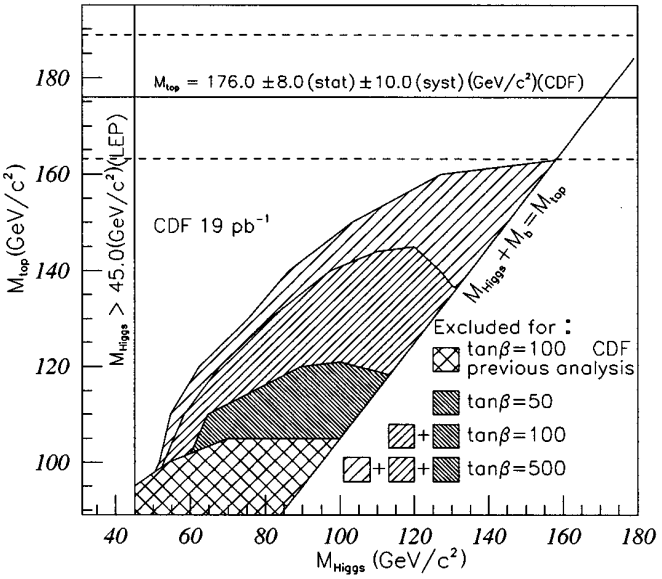

FIG. 8. Regions of the $(m_{\text{top}}, m_{\text{Higgs}})$ plane excluded at 95% C.L. for different values of tan β. The plot also shows the limit from the previous analyses [2,3].

background events. The normalization method is based on jet trigger events, but one can check for a trigger bias by removing the jet which was responsible for the trigger, and no significant effect appears. The total hadronic background is conservatively estimated to be $17.4 \pm 2.5(\text{stat}) \pm 0.6(\text{syst})$ events, based on these cross-checks.

We have compared the number of expected events for different masses of the top quark and the charged Higgs boson with and without initial-state gluon radiation in ISAJET. Half the difference between these numbers was taken as the systematic uncertainty. The mean value between the number of expected events with and without initial-state gluon radiation was taken as the number of expected events. The isolation cut is the criterion most affected by initial-state gluon radiation; the number of jets is smaller with no initial-state gluon radiation. The probability to have associated charged particles of the τ candidate mixed with a particle of another jet becomes smaller and the efficiency of the cut increases. This effect also depends on the top quark mass, since for a heavy top quark there is less energy to produce jets as a result of the initial-state gluon radiation.

The systematic uncertainty on the trigger efficiency was estimated by varying each point of the measured trigger efficiency by its uncertainty. The relative uncertainty on the number of expected events due to the systematic uncertainty in the trigger efficiency is conservatively estimated to be 5.5%. In this calculation, $m_{\text{top}}=120$ GeV/c^2 and $m_{\text{Higgs}}=100$ GeV/c^2.

The absolute energy scale uncertainty varies from $\pm 10\%$ at 8 GeV to $\pm 3\%$ at 100 GeV. In the Monte Carlo simulations, we shifted the jet energy scale by these values, and repeated the analysis, reconstructing the E_T of each jet and other relevant event parameters. We used the mean relative difference of the change in the number of expected events when the energy scale is shifted as the systematic uncertainty on the energy scale.

VIII. RESULTS

After selection, there remain 74 events from the data sample, of which a total of 19 events have a τ candidate with either one or three associated charged particles. Figure 6 shows the multiplicity distribution for the data sample and the hadronic background normalized to the data. For comparison, the plot shows the distribution from the Monte Carlo signal simulation normalized to the total integrated luminosity and added to the hadronic background estimation. The estimated total number of background events is 18.5 ± 2.6, where the error comes from adding in quadrature the systematic and statistical uncertainties.

The mass limits must take into account the uncertainties, both statistical and systematic, on the number of expected background and signal events. For a given mass point, a simple Monte Carlo simulation generates a large ensemble of trials with the numbers of expected signal and background events varying in a Gaussian fashion about the mean. In each trial it generated a number of observed events from a Poisson distribution with a mean equal to the number of signal plus background. The standard deviations of the Gaussians are the combined statistical and systematic uncertainties. The mass point can be excluded with 95% confidence if in 95% or more of the trials the total number of events exceeds the 19 events actually observed.

Figure 7 shows the resulting limit for large values of the parameter tan β, for which the branching ratios of $t \rightarrow Hb$ and $H \rightarrow \tau\nu$ approach unity. Figure 8 shows the limit for tan $\beta=50$, 100, and 500 in the plane of the top quark mass versus the charged Higgs boson mass. As the charged Higgs boson mass decreases, the missing transverse energy de-

creases on average, reducing the efficiency of the selection. Also, as the top mass increases, its production cross section decreases, and the number of expected events decreases. As the parameter tan β increases, the branching ratios of the top to charged Higgs boson and charged Higgs boson to τ both increase, allowing a better limit.

The event selection used is well optimized for large masses of the top quark and the charged Higgs boson. The present statistics exclude the region for large tan β, extending from the limit of the previous analyses just up to the region where the top mass has been measured.

ACKNOWLEDGMENTS

We thank the Fermilab staff and the technical staffs of the participating institutions for their vital contributions. This work was supported by the U.S. Department of Energy, the National Science Foundation, the Instituto Nazionale di Fisica Nucleare of Italy, the Ministry of Education, Science and Culture of Japan, the Natural Sciences and Engineering Research Council of Canada, the National Science Council of the Republic of China, the A. P. Sloan Foundation, and the Alexander von Humboldt-Stiftung.

[1] S. L. Glashow and E. E. Jenkins, Phys. Lett. B **196**, 233 (1987); V. Barger, J. L. Hewett, and R. J. N. Phillips, Phys. Rev. D **41**, 3421 (1990).
[2] F. Abe, *et al.*, Phys. Rev. Lett. **72**, 1977 (1994).
[3] F. Abe, *et al.*, Phys. Rev. Lett. **73**, 2667 (1994).
[4] D. Decamp, *et al.*, Phys. Rep. **216**, 253 (1992); P. Abreu, *et al.*, Phys. Lett. B **241**, 449 (1990); O. Adriani, *et al.*, *ibid.* **294**, 457 (1992); M. Z. Akrawy, *et al.*, *ibid.* **242**, 299 (1990).
[5] F. Abe, *et al.*, Phys. Rev. Lett. **74**, 2626 (1995); S. Abachi, *et al.*, *ibid.* **74**, 2632 (1995).
[6] F. Abe, *et al.*, Nucl. Instr. Meth. A **271**, 387 (1988).
[7] The pseudorapidity η is defined as $\eta \equiv -\ln(\tan \theta/2)$ with the angle θ between the beam axis and the direction of a particle measured assuming a z-vertex position of zero unless otherwise noted, where z is the position along the beam axis.
[8] F. Paige and S. D. Protopopescu, BNL Report No. BNL 38034, 1986 (unpublished).
[9] G. Marchesini, *et al.*, Comput. Phys. Commun. **67**, 465 (1992).
[10] E. Laenen, J. Smith, and W. L. van Neerven, Phys. Lett. B **321**, 254 (1994).
[11] F. Abe, *et al.*, Phys. Rev. D **44**, 29 (1991).